pISSN 1229-3008 eISSN 2287-6251
Progress in Superconductivity and Cryogenics
Vol.21, No.4, (2019), pp.34~38

https://doi.org/10.9714/psac.2019.21.4.034

Evaluation of the delamination strengths in differently processed practical Ag-stabilized REBCO CC tapes under transverse loading

Mark A. Diaz[a], Hyung-Seop Shin[a,*] Hongsoo Ha[b], and Sang-Soo Oh[b]

[a] *Department of Mechanical Design Engineering, Andong National University, Andong, 36729 Korea*
[b] *KERI, Changwon, 51543, Korea*

(Received 11 December2019; revised or reviewed 18 December 2019; accepted 19 December 2019)

Abstract

Multilayered high-temperature superconductor coated conductor (CC) tapes are used in an extensive range of applications and are exposed to many stresses such as hoop stress, radial/transverse tensile stress under large Lorentz forces, and thermal stress while cooling if thermal expansion properties differ. Loads induced transversely at the tape surface inevitably create delamination phenomena in the multilayered CC tapes. Thus, delamination behaviors of CC tapes along the c-axis under transverse loading conditions, which can vary based on manufacturing process and constituent layers, must be characterized for applications. The anvil test method was used to mechanically investigate the delamination characteristics of various commercially available Ag-stabilized CC tapes at room temperature and 77 K, finding superior strength at the latter. The wide variations found depended on tape structure and fabrication technique. Fractographic morphologies of delaminated tapes supported the findings under transverse loading conditions.

Keywords: delamination, coated conductor, transverse tension, mechanical delamination strength, anvil test method

1. INTRODUCTION

Multi-layered high-temperature superconductor (HTS) coated conductor (CC) tapes are extensively used in manufacturing wet wound coils, exposing the tapes to high magnetic fields. Because REBCO CC tapes show excellent performance in magnetic fields, they must sustain their superconducting properties under mechanical stresses such as thermal stress and electromagnetic stress [1-3]. In particular, the stress along the c-axis of a CC tape can cause damage of the superconducting layer due to delamination, given the uncertain behaviors at the interfaces between constituent layers while the tape cools to operating temperature, inducing a transversely applied load to the tape surface [4, 5].

It has recently been found that the electromechanical properties of HTS tapes can be reinforced electroplated layer, which adds electrical stability. With a multi-layered structure in CC tapes, factors such as differing coefficients of thermal expansion (CTEs) between the constituent layers, extreme radial forces, and other coil-related issues could influence delamination behaviors [3, 6, 7]. When CC tapes are manufactured in different ways and sizes, different delamination strengths can result, as is the case with tapes fabricated using IBAD/RCE-DR or RABiTS/MOD [6, 8]. The reinforcing layer is necessary to enhance current carrying capabilities, and the protective layer can create an imbalance in the CTEs, eventually leading to delamination.

To better understand the influences of the various stabilizing layers used in fabricating CC tapes including an efficient removal of substrate to increase the engineering current density, J_e, and to evaluate the weakest point in a multi-layered tape, delamination behaviors must be characterized. The effect of a transversely applied tension load was evaluated using an unslit 12-mm-wide CC tape, yielding a correlation that could be used in the major applications of HTS tapes. It is important to characterize their delamination behaviors under transverse loading conditions because the delamination phenomena can differ depending on the manufacturing process and the constituent layers.

In this study, an anvil test method was used to mechanically investigate the delamination characteristics in differently processed practical Ag-stabilized CC tapes obtained from various manufacturers. After the anvil tests at room temperature (RT) and 77 K, delamination morphologies were examined using energy-dispersive electron spectroscopy (EDS) and scanning electron microscopy (SEM).

* Corresponding author: hsshin@anu.ac.kr

2. EXPERIMENTAL PROCEDURE

2.1. Samples

One Ag-stabilized CC tape with un-slit edges was obtained from each of six manufacturers, and they were labelled Sample 1, 2, etc. Each was ~12 mm in width except for Sample 6, which was ~10 mm in width. Each manufacturer used their own stabilizing technique and substrate material, resulting in samples of different thicknesses (see Table 1). Each sample was cut into 50 mm lengths for mechanical delamination tests.

TABLE I
VARIATIONS IN THICKNESS BETWEEN THE COATED CONDUCTOR TAPE SAMPLES.

Sample	Sample 1	Sample 2	Sample 3	Sample 4	Sample 5	Sample 6
Fabrication process	IBAD/RCE-DR	IBAD/MOCVD	IBAD/PLD	ISD/RCE	IBAD/PLD	IBAD/PLD
Substrate thickness, μm	100	47	103	97	72	45
Ag thickness (*REBCO side*), μm	9	6.5	8	8.5	8	6.5
Ag thickness (*substrate side*), μm	6	7.2	6	5.5	7	5
Total thickness, μm	115	56	117	111	87	57

2.2. Setup for Mechanical Delamination Tests

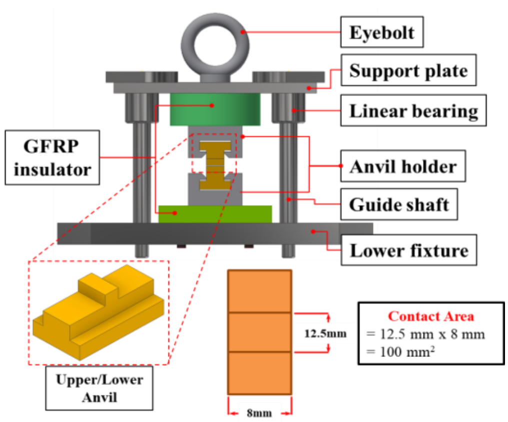

(a)

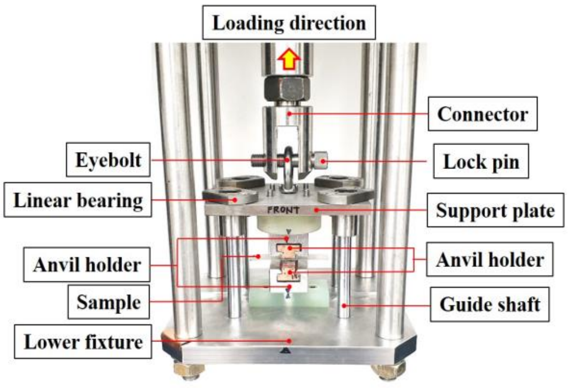

(b)

Fig. 1. (a) schematic diagram of the new testing apparatus and (b) anvil test setup for delamination test under transverse tension loading.

An anvil test method was used to conduct mechanical delamination tests. The anvils were 12.5 mm to assure that the entire width of the tape was covered, representing the actual condition in a superconducting coil application. The upper and lower copper anvils were carefully soldered at 110–120 °C to both sides of the tape sample using In-Bi solder with flux ($ZnCl_2$) [9]. During soldering, a sample mounting holder was used to ensure that the loading axis was properly aligned with the soldered sample/anvil assembly and to assure that the solder at the sample/anvil contact area was evenly distributed, a potentially important detail that assures the resultant data will be less scattered and more reliable.

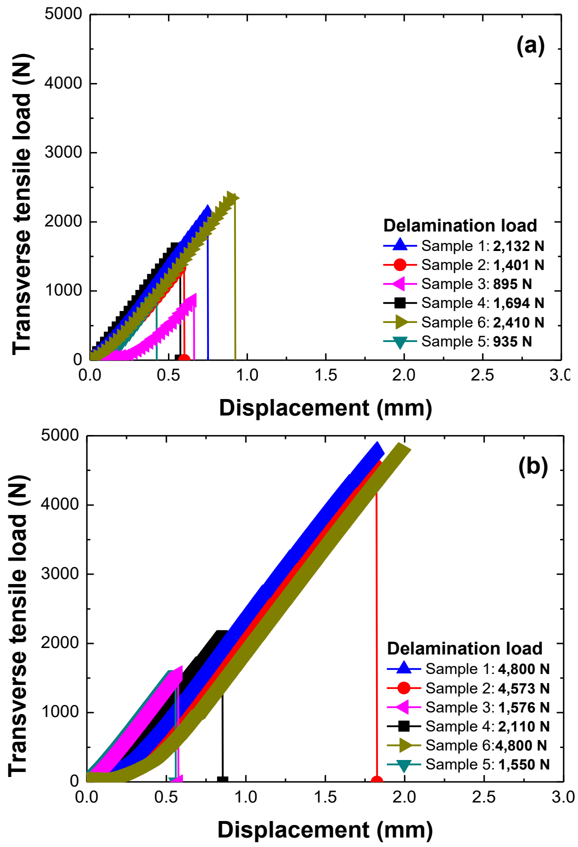

Fig. 2. Load-displacement curve of each sample at (a) room temperature and (b) 77 K.

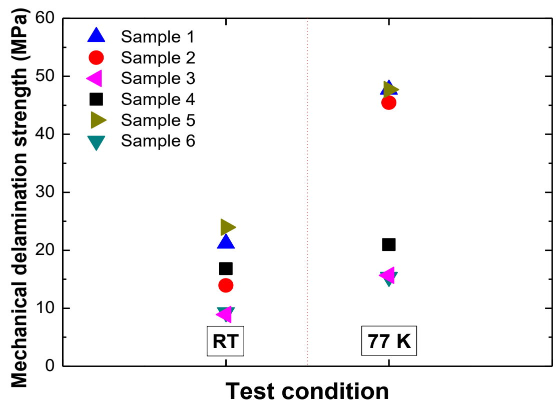

Fig. 3 Mechanical delamination strength of differently processed Ag-stabilized CC tapes obtained at each test temperature conditions.

TABLE II
DELAMINATION CHARACTERISTICS OF AG-STABILIZED COATED CONDUCTOR TAPE AT ROOM TEMPERATURE AND 77 K.

Sample	Room temperature			77 K		
	Transverse peak load (N)	Delamination strength (MPa)	Fracture description	Transverse peak load (N)	Delamination strength (MPa)	Fracture description
Sample 1	2,132	21	Totally delaminated (SC side)	4,800	48	No delamination
Sample 2	1,401	14	Totally delaminated (SC side)	4,573	45	Totally delaminated (SC side)
Sample 3	895	9	Totally delaminated (SC side)	1,576	16	Totally delaminated (SC side)
Sample 4	1,694	17	Totally delaminated (SC side)	2,110	21	Totally delaminated (SC side)
Sample 5	935	24	Totally delaminated (SC side)	4,800	48	No delamination
Sample 6	2,410	9	Totally delaminated (SC side)	1,550	15	Totally delaminated (SC side)

The flux helps equalize solder flow as it melts under the heat of the soldering iron. The soldering configuration, wherein the superconducting layer side of the CC tape faced the upper anvil, was the same for all tests of all samples.

The sample/anvil assembly was then mounted onto a revised delamination testing apparatus as illustrated in Fig. 1. The apparatus is as described elsewhere [6], except 4 guide shafts and linear bearings were introduced to prevent unwanted movements of the sample/anvil assembly and to achieve a more uniform distribution of the transverse tension load applied to the surface of the CC tape. This setup maintains good alignment between the loading axis and the sample/anvil assembly during transverse tension testing.

When a delamination fracture occurred during testing, the transverse load peaked, observable on load-displacement curves obtained at a constant cross-head velocity of 1 mm/min. The mechanical delamination strength ($\sigma_{del.}$) of each sample could be derived by dividing the peak transverse load by the upper anvil/sample contact area.

3. RESULTS AND DISCUSSION

3.1. Mechanical Delamination Strength

As shown in Fig. 2, the load-displacement curves obtained under various testing conditions reveal that the peak transverse load varied based on the sample manufacturer and test temperature. Of note, the peak load was greater at 77 K than at RT. Scattering was greater among the samples tested at 77 K.

Fig. 3 shows that $\sigma_{del.}$ was superior at 77 K compared to RT and that scattering depended on test temperature. Wider scattering at 77 K indicates that the thermal cycle influenced σ_{del}.

At 77 K, greater values for $\sigma_{del.}$ were found for Samples 1, 2, and 5 (45 to 48 MPa) compared to Samples 3 and 6. The difference might be the result of weak adhesion between the REBCO/buffer layers and the substrate. This shows that $\sigma_{del.}$ was not significantly influenced by the thickness of the Ag layer meant to protect the REBCO layer. Therefore, the delamination phenomena could be attributed to differences in CTE across the constituent layers upon thermal cycling [2], which degrades the current-carrying capabilities of CC tapes.

3.2. Morphologies of Delaminated Samples

After transverse tension tests, the morphologies of the delaminated samples were examined to clarify the delamination mechanism. Results are shown in Table 2. Samples tested at RT showed complete delamination of the REBCO superconducting side. However, at 77 K, some samples (e.g., 1 and 5) showed higher delamination strengths and did not delaminate even at the full load capacity (5 kN) of the testing apparatus.

The delaminated part, the superconducting layer particularly, was used to carry out element mapping using EDS or energy dispersive X-ray spectroscopy in conjunction with SEM, as shown in Fig. 4. The resultant colored maps reveal the location and intensity of each element in the SEM image. Fig. 4(a) shows the EDS maps of samples exhibiting lower values for σ_{del}. The weakest part of most of the samples that delaminated and had lower strengths was in the interface between the superconductor/buffer layer and the substrate. For example, nickel (Ni), the greatest portion of the Hastelloy C-276 alloy [10], was found to be quite prevalent. On the other hand, barely a trace can be seen in the superconducting layer where there is also a minimal presence of solder (In).

After analyzing the delaminated portions of Ag-stabilized CC tapes with greater values of $\sigma_{del.}$, those with mixed delamination sites probably failed at the Ag/REBCO interface [9]. Some showed little presence of the REBCO film (Fig. 4(b)). When the substrate dominated at the delaminated sites, the intensities of both Ag and In solder were minimal.

At RT, similar delamination sites were seen on the superconducting side, indicating that all samples were fully delaminated and lost every trace of the REBCO layer. Further investigations utilizing multiple tests will reinforce these findings.

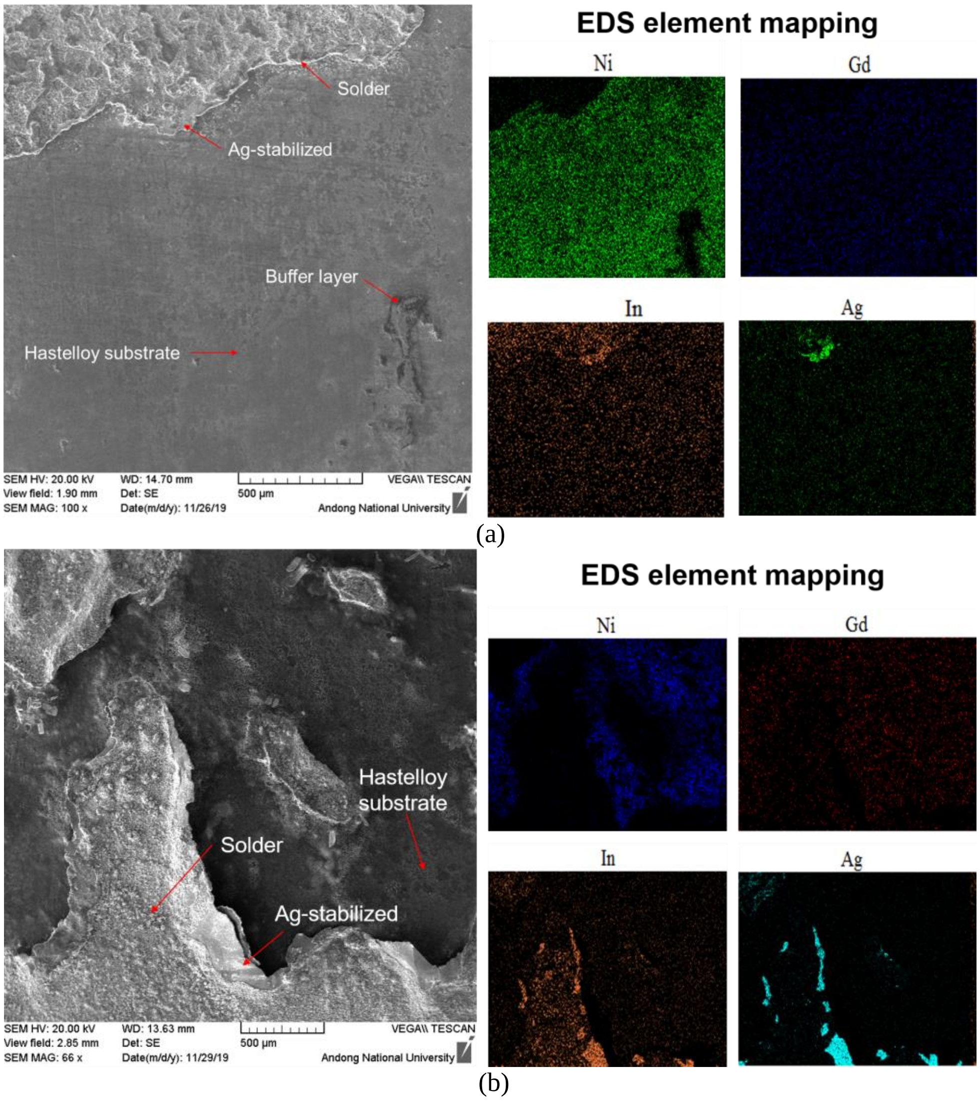

Fig. 4. Fracture morphologies of Ag-stabilized coated conductor tapes after delamination tests and SEM-EDS element mapping for (a) a lower delamination strength sample (Sample 4) and (b) a higher strength sample (Sample 2).

4. CONCLUSION

Mechanical delamination strengths of 12-mm wide Ag-stabilized CC tapes supplied by various manufacturers were tested using an anvil method under transverse tensile loading at RT and 77 K. The delamination occurred at the superconducting layer side and the weakest points in multilayered CC tapes, mainly at the interfaces between the REBCO superconducting/buffer layer and the substrate no matter the test conditions. The thickness of the Ag stabilizer did not appreciably influence delamination behaviors at 77 K. Variations occurred due to weak interfaces, depending on the structure and fabrication technique of the sample.

ACKNOWLEDGMENT

This research was supported by the Korea Electric Power Corporation (Grant No. R18XA03) and by a grant from the National Research Foundation of Korea (NRF-2017-001901) funded by the Ministry of Science and ICT (MSIT), Republic of Korea. The authors express their thanks to Dr. M. de Leon for his assistance during SEM/EDX observations.

REFERENCES

[1] H. Miyazaki, et al., “Degradation-free impregnated YBCO pancake coils by decreasing radial stress in the windings and method for evaluating delamination strength of YBCO-coated conductors,” *IEEE Trans. Appl. Supercond.*, vol. 24, pp. 4600905, 2014.

[2] T. Takematsu, et al., “Degradation of the performance of a YBCO-coated conductor double pancake coil due to epoxy impregnation,” *Physica C*, vol. 470, pp. 674-677, 2010.

[3] S. Muto, S. Fujita, K. Akashi, T. Yoshida, Y. Iijima, and K. Naoe, “Evaluation of actual delamination strength of REBCO-coated conductors based on the Weibull analysis considering size effect,” *IEEE Trans. Appl. Supercond.*, vol. 28, pp. 6601004, 2018.

[4] Y. Zhang, et al., “Adhesion strength study of IBAD-MOCVD-based 2G HTS wire using a peel test,” *Physica C*, vol. 473, pp. 41-47, 2012.

[5] D. C. van der Laan, et al., “Delamination strength of YBCO coated conductors under transverse tensile stress,” *Supercond. Sci. Technol.*, vol. 20, pp. 765-770, 2007.
[6] A. Gorospe, A. Nisay, and H. S. Shin, “Delamination behavior of differently copper laminated REBCO coated conductor tapes under transverse loading,” *Physica C*, vol. 504, pp. 47-52, 2014.
[7] H. S. Shin, “Evaluation of delamination characteristics in GdBCO CC tapes under transverse load using anvil test method for various anvil contact configuration,” *Supercond. Sci. Technol.*, vol. 32, pp. 1033, 2019.
[8] M. Sugano, T. Nakamura, T. Manabe, K. Shikimachi, N. Hirano, and S. Nagaya, “The intrinsic strain effect on critical current under a magnetic field parallel to the c-axis for a MOCVD-YBCO-coated conductor,” *Supercond. Sci. Technol.*, vol. 21, no.11, 2008.
[9] A. Gorospe, A. Nisay, and J. R. Dizon, “Delamination behavior of GdBCO coated conductor tapes under transverse tension,” *Physica C*, vol. 494, pp. 163-167, 2013.
[10] https://www.haynesintl.com/alloys/alloy-portfolio_/Corrosion-resistant-Alloys/HASTELLOY-C-276-Alloy/principal-features.aspx